Outage Probability Analysis of UAV Assisted Satellite-Terrestrial Network

Tao Teng, Xiangbin Yu(✉), Xiaomin Chen, Kai Yu, and Guangying Wang

College of Electronic and Information Engineering,
Nanjing University of Aeronautics and Astronautics, Nanjing 211106, China
tengtaon@163.com, yxb_xwy@hotmail.com, chenxm402@nuaa.edu.cn,
yukai152163@163.com, wanggy2010@qq.com

Abstract. Satellite and UAV (unmanned aerial vehicle) communication are two vital techniques to support the upcoming 5G and beyond 5G network. Based on this, the paper considers a downlink UAV assisted hybrid satellite-terrestrial network under cognitive radio communication (HSTCN), a framework consisting of a hovering UAV and terrestrial distributed antenna system (DAS) is proposed, which is novel and complex. Our goal is to analyze the outage probability (OP) of satellite user under cognitive radio terrestrial network interference, in which the decode-and-forward UAV relay is applied to help signal transmission. The approximated closed-form outage probability is derived, experimental results are performed to demonstrate the correctness of the proposed OP results and reveal the impact of different system parameters on the satellite-terrestrial model.

Keywords: Distributed antenna system · Shadowed Rician fading · UAV · Cognitive radio · Outage probability

1 Introduction

In the age of 5G, more and more communication devices, accessed to terrestrial network, congest the communication [1,2]. Satellite and flying vehicles, such as unmanned aerial vehicles(UAV), airplanes, are applied to expanding terrestrial communication coverage, providing seamless connectivity and so on [3–6].

The idea of a hybrid satellite-terrestrial cognitive network (HSTCN) was established for satellite network integrating into terrestrial network, the satellite is licensed in air-to-ground network to operate in the same frequency band so that spectrum management works [7–12]. Yuhan Ruan et al. in [13] investigated the outage probability(OP) of an integral satellite-terrestrial network with intra-cell interference. Oluwatayo Y. Kolawole et al. in [14] studied the OP and the spectral efficiency of the proposed HSTCN where satellite network shares resources with terrestrial network. Kang An et al. in [15] researched the physical layer security of the proposed HSTCN, the optimal beamforming and

M. Guan and Z. Na (Eds.): MLICOM 2020, LNICST 342, pp. 359–370, 2021.
https://doi.org/10.1007/978-3-030-66785-6_38

power allocation algorithm was designed. Xingwang Li et al. in [16] proposed an unified framework for hybrid satellite/UAV terrestrial non orthogonal multiple access(NOMA) network, the approximate closed-form expression of the OP was obtained. Based on the approximate OP expression, the location optimization of UAV was analyzed. Xiaokai Zhang et al. in [17] investigated the OP and the ergodic capacity of NOMA based on the hybrid satellite-terrestrial network. The terrestrial network is used as relay cooperating with primary satellite network. Silin Xie et al. in [18] derived the closed-form expression of the OP with NOMA transmission. Imperfect channel state information was considered at all nodes.

The integration of the satellite and UAV could be applied to serve the remote areas as well as the disaster areas. UAV often acts as a relay to help satellite signal transmitting or terrestrial network transmitting. Research the architecture of [19–22] satellite-terrestrial network with the aid of the UAV. Xiaomin Chen et al. researched the multi-hop UAV assisted channel model establishment. With the proposed model, the OP, bit error rate and channel capacity are analyzed and derived [23,24] . Optimization problems such as maximizing the system transmitting rate, finding the optimal UAV trajectory, power allocation of both the satellite and UAV groups are provided. It can be found that UAV fits well with the satellite-terrestrial network and the power allocation association is vital in the integration of satellite-UAV networks. Pankaj K. Sharma et al. in [25] investigated a hybrid satellite terrestrial network with decode-and-forward(DF) protocol and stochastic geometry. The outage probability under opportunistic UAV relay selection was provided, the secure outage probability of the proposed system model was analyzed in [26] either. Ting Qi et al. integrated NOMA into satellite-UAV network, both the outage probability and the power allocation algorithm were proposed to guarantee the fairness between two NOMA users [27].

Motivated by the aforementioned papers, in this paper, we construct a novel satellite-terrestrial network which consists of a UAV and a single cell DAS. Cognitive radio with underlay mode is applied to integrate the satellite with the terrestrial network. Outage probability is chosen to analyze the system performance. We make the following contributions: (1) A novel framework containing UAV and DAS is built for downlink performance analysis. (2) Cognitive radio is applied for satellite-terrestrial network integration, which makes the outage probability derivation difficult. (3) An approximated closed-form OP is derived, the related simulation is implemented to analyze the proposed model.

2 System Model

As shown in Fig. 1, we consider a downlink UAV assisted HSTCN which consists of one geosynchronous orbit(GEO) satellite s, one UAV relay g, N_t DA ports $b_1, \cdots, b_{N_t}$, one primary terrestrial user (PTU) pu, and one secondary satellite user (SSU) su. Satellite s communicates with SSU with the help of UAV by using DF protocol. At the same time, DA ports transmit signals to PTU, which causes interference to SSU under the same spectrum. For ease of analysis, all of the nodes are equipped with one antenna. Besides, by supposing a poor channel condition between satellite and SSU, the direct link is blocked.

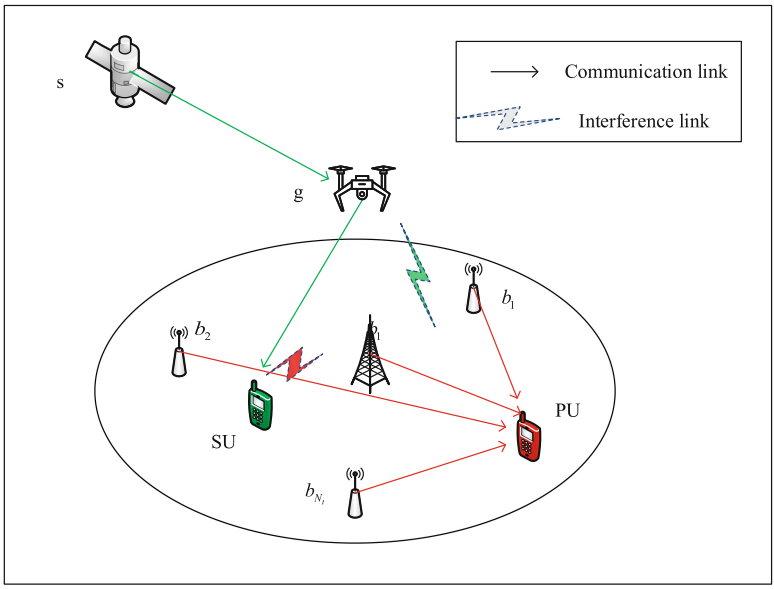

Fig. 1. System model

2.1 Signal Model

The communication between s and SSU takes place in a two-time phase. The received signal at UAV in the first phase can be given by

$$y_g = \sqrt{p_s}\sqrt{G_{s,g}}h_{s,g}x_s + n_g, \tag{1}$$

At the second time slot, g decodes the received signal y_g and then retransmits to SSU. Thus, the received signal at SSU is written as

$$y_{su} = \sqrt{p_g}\sqrt{G_{g,su}}h_{g,su}x_s + \sum_{i=1}^{N_t}\sqrt{p_{bi}}\sqrt{G_{bi,su}}h_{bi,su}s_{bi} + n_{su}. \tag{2}$$

where $n_g \sim CN\left(0, \sigma_g^2\right)$ and $n_{su} \sim CN\left(0, \sigma_{su}^2\right)$. To ensure the interference at PTU beyond to I_{th}, the transmitting power at UAV must satisfy

$$p_g = \min\left\{\frac{I_{th}}{|h_{g,pu}|^2}, p_{g\max}\right\}, \tag{3}$$

where I_{th} means interference-power threshold. By combining (2) with (3), the SINR at SSU can be formulated as

$$\gamma_{su} = \frac{\min\left\{\bar{\gamma}_s G_{s,g}|h_{s,g}|^2, G_{g,su}|h_{g,su}|^2 \min\left\{\frac{\bar{\gamma}_{th}}{|h_{g,pu}|^2}, \bar{\gamma}_{g\max}\right\}\right\}}{\sum_{i=1}^{N_t}\bar{\gamma}_{bi}G_{bi,su}|h_{bi,su}|^2 + 1}. \tag{4}$$

where $\bar{\gamma}_s = p_s/\sigma_g^2, \bar{\gamma}_{th} = I_{th}/\sigma_{su}^2, \bar{\gamma}_{bi} = p_{bi}/\sigma_{su}^2$.

2.2 Channel Model

The traditional satellite-terrestrial model includes the Loo model, Corazza model, etc. [28]. However, the theoretical probability density function(PDF) is complex. Authors Ali Abdi etc. in [29] proposed a simple model for Land Mobile Satellite(LMS) Channel named Shadowed Rician(SR) model with parameters (b_s, m_s, Ω_s). Under the situation of integer values m_s, references [30,31] proposed a simple SR PDF expression, which can be written as

$$f(x) = \alpha \sum_{k=0}^{m_s-1} \zeta(k)\, x^k \exp(-(\beta-\delta)\, x). \tag{5}$$

where $\alpha = \left[(2b_s)^{m_s+1} {m_s}^{m_s}\right] \Big/ [(2b_s m_s + \Omega_s)^{m_s}]$, $\delta = \Omega_s / [2b_s\,(2b_s m_s + \Omega_s)]$. $\beta = 1/(2b_s)$, Ω_s is the average power of the shadow fading, $2b_s$ represents the average power of the multipath, $m_s \in (0, \infty)$ means the fading parameter of the shadow fading. $\zeta(k) = \left[(-1)^k (1-m_s)_k \delta^k\right] \Big/ \left[(k!)^2\right]$, $(\cdot)_p$ is the Pochhammer symbol.

The channel fading between UAV and PTU/SSU is modelled as Rician fading. The PDF and cumulative distribution function(CDF) of the Rician channel can be written as

$$f(x) = (1+K) \exp(-((1+K)\, x + K))\, I_0\left(\sqrt{4K\,(K+1)\, x}\right), \tag{6}$$

$$F(x) = 1 - Q_1\left(\sqrt{2K}, \sqrt{2\,(1+K)\, x}\right). \tag{7}$$

where K is Rician factor, $Q_M(a, b)$ means the Marcum Q function with order M. Besides, the channel between DA ports and SSU is assumed as Nakagami fading. Let $G_{s,g} = L_{s,g} G_s G_g \left(J_1(x)/(2x) + (36 J_3(x))/x^3\right)$ denote the propagation gain including free-space loss and antenna gain at both the satellite and the UAV, which can be described in [14]. Let $G_{g,su}$ and $G_{bi,su}$ be the antenna gain between the UAV/DA ports to SU, which has been described as $G_{g,su} = G_g G_{su} L_{g,su}$, $G_{bi,su} = G_{bi} G_{su} L_{bi,su}$ with $L_{\varsigma,su} = \left(h_{\varsigma,su}^2 + z_{\varsigma,su}^2\right)^{-\alpha/2}$, $\varsigma \in \{g, b_i\}$ respectively. $h_{\varsigma,su}$ is the difference in height between g/b_i and SSU, $z_{\varsigma,su}$ denotes the difference on the ground plane between SSU and the projection of ς. α means the path loss index. Based on the above definitions, the outage probability can be derived in the following section.

3 Outage Probability Analysis

Outage probability is defined as the probability that the transmitting link capacity falls below the needed user rate, which also can be written as:

$$F_1(x) = \Pr\left\{ \frac{\min\left\{\bar{\gamma}_s G_{s,g}|h_{s,g}|^2, G_{g,su}|h_{g,su}|^2 \min\left\{\frac{\bar{\gamma}_{th}}{|h_{g,pu}|^2}, \bar{\gamma}_{g\max}\right\}\right\}}{\sum_{i=1}^{N_t} \bar{\gamma}_{bi} G_{bi,su}|h_{bi,su}|^2 + 1} \le x \right\}$$
$$= \int_0^\infty F_2(xu) f_7(u)\, du. \tag{8}$$

where $F_2(x)$ denotes the probability that the numerator of (4) falls below x. To proceed further, $F_2(x)$ can be decomposed as:

$$F_2(x) = \Pr\left\{ \min\left\{\bar{\gamma}_s G_{s,g}|h_{s,g}|^2, G_{g,su}|h_{g,su}|^2 \min\left\{\frac{\bar{\gamma}_{th}}{|h_{g,pu}|^2}, \bar{\gamma}_{g\max}\right\}\right\} \le x \right\}$$
$$= F_3(x) + F_4(x) - F_3(x) F_4(x), \tag{9}$$

As is derived in [30], the closed-form expression of $F_3(x)$ is shown as:

$$F_3(x) = \Pr\left\{\bar{\gamma}_s G_{s,g}|h_{s,g}|^2 \le x\right\}$$
$$= 1 - \alpha \sum_{k_5=0}^{m_s-1} \zeta(k) \sum_{p=0}^{k_5} \frac{k_5!}{p!} (\beta-\delta)^{-(k_5+1-p)} \left(\frac{x}{\bar{\gamma}_s G_{s,g}}\right)^p \exp\left(-\frac{x(\beta-\delta)}{\bar{\gamma}_s G_{s,g}}\right), \tag{10}$$

Moreover, $F_4(x)$ can be decomposed into two independent outage probability items, which gives the following equation:

$$F_4(x) = \Pr\left(\min\left\{\frac{\bar{\gamma}_{th}}{|h_{g,pu}|^2}, \bar{\gamma}_{g\max}\right\} G_{g,su}|h_{g,su}|^2 \le x\right)$$
$$= \Pr\left\{\frac{\bar{\gamma}_{th}}{|h_{g,pu}|^2} G_{g,su}|h_{g,su}|^2 \le x, \frac{\bar{\gamma}_{th}}{|h_{g,pu}|^2} < \bar{\gamma}_{g\max}\right\}$$
$$+ \Pr\left\{\frac{\bar{\gamma}_{th}}{|h_{g,pu}|^2} > \bar{\gamma}_{g\max}, \bar{\gamma}_{g\max} G_{g,su}|h_{g,su}|^2 \le x\right\}, \tag{11}$$

By applying (6), (7) into (11) and utilizing [32] (Eq. 8), the closed-form expression of $F_4(x)$ is obtained. Then putting $F_4(x)$ together with $F_3(x)$ into $F_2(x)$, with variable substitution and simplification, the expression of $F_2(x)$ is written as:

$$F_2(x) = 1 - \sum_{k_1=0}^{\infty}\sum_{k_2=0}^{\infty}\sum_{k_5=0}^{m_s-1}\sum_{p=0}^{k_5}\Psi(k_1,k_2,k_5,p)\frac{x^{p+k_2}\exp\left(-\frac{x(\beta-\delta)}{\bar{\gamma}_s G_{s,g}}\right)}{\left[\frac{(1+K_{su})x}{G_{g,su}\bar{\gamma}_{th}}+(1+K_{pu})\right]^{k_2+k_1+1}}\times$$
$$\Gamma\left(k_2+k_1+1,\frac{(1+K_{su})x}{G_{g,su}\bar{\gamma}_{g\max}}+\frac{(1+K_{pu})\bar{\gamma}_{th}}{\bar{\gamma}_{g\max}}\right)-\sum_{k_4=0}^{\infty}\sum_{k_6=0}^{m_s-1}\sum_{p_1=0}^{k_6}\Psi(k_4,k_6,p_1)\times$$
$$x^{k_4+p_1}\exp\left(-\left(\frac{\beta-\delta}{\bar{\gamma}_s G_{s,g}}+\frac{1+K_{su}}{\bar{\gamma}_{g\max}G_{g,su}}\right)x\right). \tag{12}$$

where K_{su} and K_{pu} denote the Rician fading parameters of $|h_{g,su}|^2$ and $|h_{g,pu}|^2$ respectively. $\Psi(k_1,k_2,k_5,p)$ and $\Psi(k_4,k_6,p_1)$ are given as follows:

$$\Psi(k_1,k_2,k_5,p) = \exp(-K_{su}-K_{pu})\,\alpha\frac{\zeta(k_5)\,k_5!(\beta-\delta)^{-(k_5+1-p)}}{p!(\bar{\gamma}_s G_{s,g})^p}\times$$
$$\frac{(K_{pu}+1)^{k_1+1}(K_{pu})^{k_1}}{k_1!k_1k_2!}\left(\frac{1+K_{su}}{G_{g,su}\bar{\gamma}_{th}}\right)^{k_2}\sum_{k_0=0}^{\infty}\frac{{K_{su}}^{k_0+k_2}}{(k_0+k_2)}, \tag{13}$$

$$\Psi(k_4,k_6,p_1) = \left[1-Q_1\left(\sqrt{2K_{pu}},\sqrt{\frac{2(1+K_{pu})\bar{\gamma}_{th}}{\bar{\gamma}_{g\max}}}\right)\right]\exp(-K_{su})\times$$
$$\frac{\alpha\zeta(k_6)}{k_4!}\left(\frac{K_{su}(1+K_{su})}{\bar{\gamma}_{g\max}G_{g,su}}\right)^{k_4}\sum_{k_3=0}^{\infty}\frac{{K_{su}}^{k_3}}{(k_3+k_4)}\frac{k_6!(\beta-\delta)^{-(k_6+1-p_1)}}{p_1!(\bar{\gamma}_s G_{s,g})^{p_1}}. \tag{14}$$

As is discussed in [33], the PDF of the denominator in (4), denoted by $f_7(x)$, can be approximated as

$$f_7(x) = x^{m_b-1}\frac{e^{-x/\Omega_b}}{{\Omega_b}^{m_b}\Gamma(m_b)}. \tag{15}$$

where the shape parameter $m_b = \left(\sum_{i=1}^{N_t}\bar{\gamma}_{bi}G_{bi,su}\Omega_{su}\right)^2 \Big/ \left(\sum_{i=1}^{N_t}\bar{\gamma}_{bi}^2 G_{bi,su}^2\frac{\Omega_{su}^2}{m_{su}}\right)$, the scale parameter $\Omega_b = \left(\sum_{i=1}^{N_t}\bar{\gamma}_{bi}^2 G_{bi,su}^2\frac{\Omega_{su}^2}{m_{su}}\right)\Big/\left(\sum_{i=1}^{N_t}\bar{\gamma}_{bi}G_{bi,su}\Omega_{su}\right)$ respectively. Thus, by substituting (12), (15) into (8) ,the OP of the SSU can be transformed as:

$$F_1(x) = I_1 - I_2 - I_3. \tag{16}$$

Here we need to calculate I_1, I_2, I_3 in turn. The closed-form expression of I_1 can be expressed as:

$$I_1 = \int_0^{\infty}\frac{u^{m_b-1}e^{-u/\Omega_b}}{\Omega_b^{m_b}\Gamma(m_b)}du = 1, \tag{17}$$

We now derive the analytical expression of I_2. First, the incomplete Gamma function $\Gamma(1+n,x)$ can be transformed as the finite series expansion of polynomial expression [32] (Eq. 8.352.7), then $(1+u)^k$ is approximated to u^k for ease of computational complexity. Finally, I_2 can be derived with the aid of [32] (Eq. 7.813.1).

$$I_2 \approx \sum_{k_1=0}^{\infty}\sum_{k_2=0}^{\infty}\sum_{k_5=0}^{m_s-1}\sum_{p=0}^{k_5}\Psi(k_1,k_2,k_5,p)\frac{(k_2+k_1)!}{\Omega_b^{m_b}\Gamma(m_b)}\left(\frac{\bar{\gamma}_{th}}{\bar{\gamma}_{g\max}}\right)^{k_2+k_1+1}x^{p+k_2}\times$$
$$\exp\left(-\left[\omega_s x+\omega_{su}x+\omega_{pu}\right]\right)\sum_{m_q=0}^{k_2+k_1}\frac{\left[\omega_{su}x+\omega_{pu}\right]^{m_q-k_2-k_1-1}}{m_q!}\frac{\left[\omega_{su}x+\omega_s x+\frac{1}{\Omega_b}\right]^{-(p+k_2+m_b)}}{\Gamma(k_2+k_1+1-m_q)}\times$$
$$G_{21}^{12}\left(\frac{\omega_{su}x}{\left[\omega_{su}x+\omega_{pu}\right]\left[\omega_{su}x+\omega_s x+\frac{1}{\Omega_b}\right]}\middle|\begin{matrix}1-p-k_2-m_b, m_q-k_2-k_1\\ 0\end{matrix}\right), \tag{18}$$

By substituting the last term of (12) and the formula of (15) into (8), with the same operation like I_2, $(1+u)^k$ is approximated to u^k, the integration of I_3 can be derived. Thus, the analytical closed form expression of I_3 is given by

$$I_3 \approx \sum_{k_4=0}^{\infty}\sum_{k_6=0}^{m-1}\sum_{p_1=0}^{k_6}\Psi(k_4,k_6,p_1)\,x^{k_4+p_1}\frac{\exp\left(-\left(\frac{\beta-\delta}{\bar{\gamma}_s G_{s,g}}+\frac{1+K_{su}}{\bar{\gamma}_{g\max}G_{g,su}}\right)x\right)}{{\Omega_b}^{m_b}\Gamma(m_b)}\times$$
$$\frac{\Gamma(k_4+p_1+m_b)}{\left(\frac{\beta-\delta}{\bar{\gamma}_s G_{s,g}}+\frac{1+K_{su}}{\bar{\gamma}_{g\max}G_{g,su}}\right)^{k_4+p_1+m_b}}. \tag{19}$$

where $\omega_{su}=(1+K_{su})/(G_{g,su}\bar{\gamma}_{g\max})$, $\omega_{pu}=[(1+K_{pu})\bar{\gamma}_{th}]/\bar{\gamma}_{g\max}$ and $\omega_s=(\beta-\delta)/(\bar{\gamma}_s G_{s,g})$. From the above analysis, OP at SSU can be computed with (17), (18), and (19). To obtain more insights, the numerical results are provided for OP analysis in the next section.

4 Numerical Results

In the simulations, the concrete antenna gain parameters and the channel fading parameters are given in Table 1. Besides, the location of UAV, DA ports and terrestrial users are defined in Table 2. The theoretical curves are obtained using (16)–(19) with the substitution of finite terms(such as 15 terms) We found that the theoretical results agree well with Monte Carlo simulation. The polar coordinates of DA prots are set as$\{2R/3,[2\pi(j-1)]/(N_t-1)\}$, $j=2,\cdots,N_t$, where one DA port is located in the center. Shadowed Rician parameters are set as $(b_s,m_s,\Omega_s)=(0.251,5,0.279)$, Rician factors at SSU/PTU are set as 2/1 respectively. $\sigma_g^2=\sigma_{su}^2=N_0$, Nakagami fading parameters are $(m_{su},\Omega_{su})=(1,1)/(2,5)$ respectively.

Figure 2 shows the results of the OP versus $p_{g\max}$. The transmitting power of satellite and DA ports are set as its maximum transmitting power. It can be found that the value of OP decreases when $p_{g\max}$ increases, this is because increasing the value of $p_{g\max}$ can enlarge the SINR of the total system. The

Table 1. Simulation parameters

Notation	Value
Carrier bandwidth W	500 MHz
Carrier frequency f_c	20 GHz
The variance of AWGN N_0	−110 dBm
Antenna gain $G_s/G_g/G_u$ /G_{bi}	53 dB/15 dB/4.8 dB/15 dB
3 dB angle of the UAV $\phi_{3\,dB}$	0.4°
Off axis angle of the UAV ϕ	0.6°
Maximum transmitting power $p_s/p_g/p_{bi}$(dB)	50 dB/40 dB/20 dB

Table 2. Terrestrial network parameters

Notation	Value
Node Height $h_g/h_{bi}/h_u$	200 m/30 m/0 m
Radius of the DAS R	1000 m
Pass loss index α	4
Projection location of the UAV/SU/PU	(0,0)/(500,π/3)/(300,3π/2)

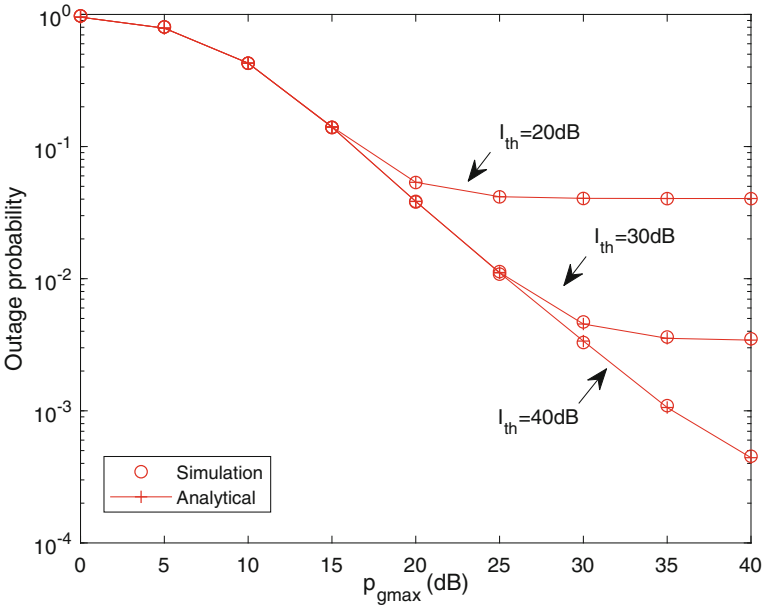

Fig. 2. OP with different cognitive threshold

curve of OP trends to be saturated eventually. It also can be found that when I_{th} increases, the value of OP decreases, when $I_{th} = 50$dB, the curve of OP decreases monotonically. Thus, when the interference power constraint is stricter, the OP of SSU is worse to protect the common communication between DAS and PTU.

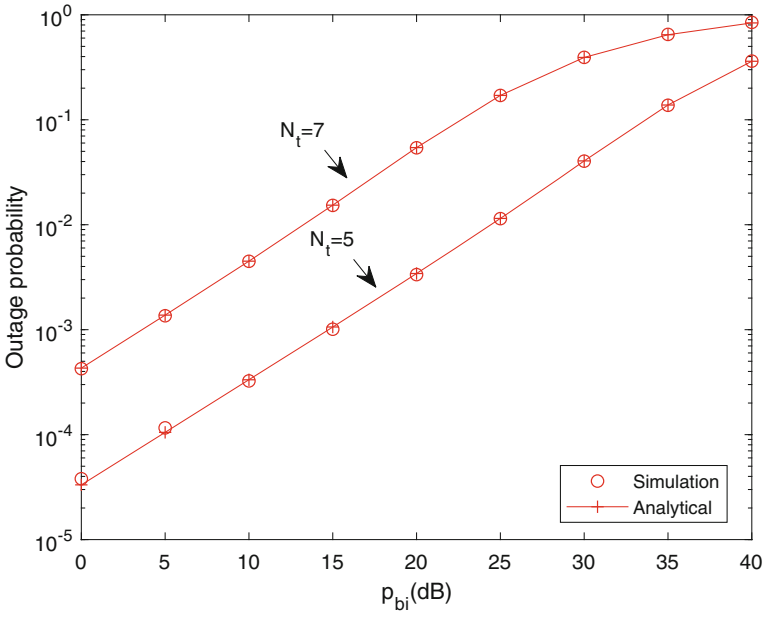

Fig. 3. OP with different number of DA ports

Figure 3 describes the OP for changing p_{bi} as well as the number of DA ports. It is obvious that when the transmitting power of DA port increases, the performance of OP decreases. This is because the transmitting signal of DA ports could cause interference to SSU. Moreover, if we increase the number of the DA ports, the OP at the SU will be worse. The reason for this phenomenon is that when the number of the DA ports increases, the condition of terrestrial communication becomes better, which causes the communication quality at SSU be worse. Besides, we can find that the approximated closed-form expression is still accurate despite of the approximation closed-form OP derivation in (18) and (19).

Finally, we investigate the outage probability performance based on the fixed satellite transmitting power and fixed UAV transmitting power(50 dB and 40 dB respectively)in Fig. 4. It is obvious that the value of the system OP increases when the transmitting power of the DAS increases. Moreover, when the transmitting channel at the terrestrial network become better, the system performance becomes worse than the previous. The main idea of Fig. 3 and Fig. 4 is

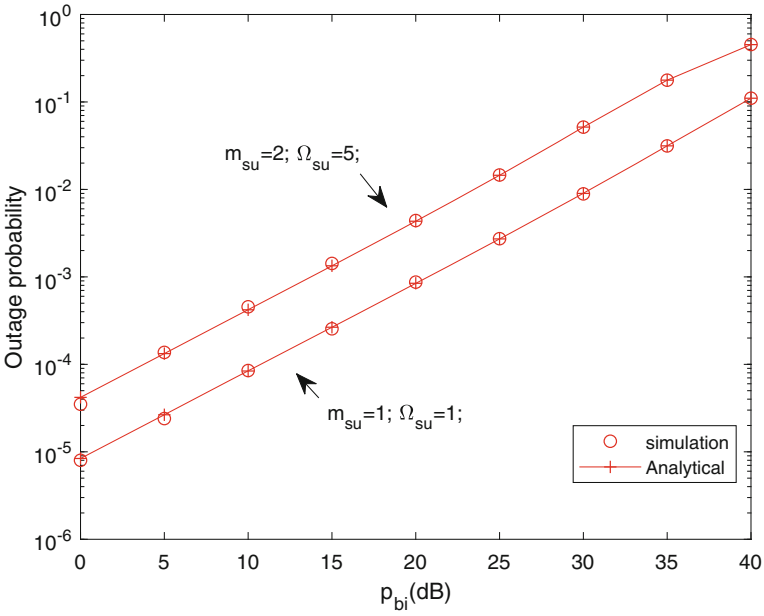

Fig. 4. OP with different values of m_{su}, Ω_{su}

illustrating the consequences of the terrestrial DAS network towards satellite communication. However, even if the proposed HSTCN needs to make a balance between satellite communication and the terrestrial network, air-ground integration did improve the total system transmission efficiency and expand the system coverage area. Several optimization problems for this model can be conducted to enhance system performance.

5 Conclusion

This paper presents a novel HSTCN model, where the framework containing UVA and DAS is set as terrestrial network. With mathematical derivation and integration operation, the closed-form OP expression of the satellite user is researched in this model. Compared with the existing work, our model is more complex and may contribute to the investigation of Satellite-UAV communication in the future. However, there are also some limitations in this paper, for example, the locations of the SSU, PTU, and the UAV are fixed, the asymptotic expression is also needed for OP performance analysis.

Acknowledgment. This work was supported in part by the National Key Scientific Instrument and Equipment Development Project under Grant No. 61827801 and in part by Aeronautical Science Foundation of China, No. 201901052001 and Postgraduate Research and Practice Innovation Program of Jiangsu Province (KYCX20-0202).

References

1. Tian, J., Zhang, H., Wu, D., Yuan, D.: QoS-constrained medium access probability optimization in wireless interference-limited networks. IEEE Trans. Commun. **66**(3), 1064–1077 (2017)
2. Qiao, J., Alouini, M.-S.: Secure transmission for intelligent reflecting surface-assisted mmwave and terahertz systems. arXiv preprint arXiv:2005.13451 (2020)
3. Vondra, M., Ozger, M., Schupke, D., Cavdar, C.: Integration of satellite and aerial communications for heterogeneous flying vehicles. IEEE Netw. **32**(5), 62–69 (2018)
4. Bai, L., et al.: Channel modeling for satellite communication channels at q-band in high latitude. IEEE Access **7**, 137691–137703 (2019)
5. Simunek, M., Font, F.P., Pechac, P.: The UAV low elevation propagation channel in urban areas: statistical analysis and time-series generator. IEEE Trans. Antennas Propag. **61**(7), 3850–3858 (2013)
6. Giambene, G., Kota, S., Pillai, P.: Satellite-5G integration: a network perspective. IEEE Network **32**(5), 25–31 (2018)
7. An, K., et al.: Performance analysis of multi-antenna hybrid satellite-terrestrial relay networks in the presence of interference. IEEE Trans. Commun. **63**(11), 4390–4404 (2015)
8. Lagunas, E., Sharma, S.K., Maleki, S., Chatzinotas, S., Ottersten, B.: Resource allocation for cognitive satellite communications with incumbent terrestrial networks. IEEE Trans. Cogn. Commun. Netw. **1**(3), 305–317 (2015)
9. Maleki, S., Chatzinotas, S., Krause, J., Liolis, K., Ottersten, B.: Cognitive zone for broadband satellite communications in 17.3c17.7 GHz band. IEEE Wireless Communications Letters **4**(3), 305–308 (2015)
10. Liang, T., An, K., Shi, S.: Statistical modeling-based deployment issue in cognitive satellite terrestrial networks. IEEE Wirel. Commun. Lett. **7**(2), 202–205 (2018)
11. Vassaki, S., Poulakis, M.I., Panagopoulos, A.D., Constantinou, P.: Power allocation in cognitive satellite terrestrial networks with QoS constraints. IEEE Commun. Lett. **17**(7), 1344–1347 (2013)
12. Wang, L., Li, F., Liu, X., Lam, K., Na, Z., Peng, H.: Spectrum optimization for cognitive satellite communications with cournot game model. IEEE Access **6**, 1624–1634 (2018)
13. Ruan, Y., Li, Y., Wang, C.-X., Zhang, R., Zhang, H.: Outage performance of integrated satellite-terrestrial networks with hybrid CCI. IEEE Commun. Lett. **21**(7), 1545–1548 (2017)
14. Kolawole, O.Y., Vuppala, S., Sellathurai, M., Ratnarajah, T.: On the performance of cognitive satellite-terrestrial networks. IEEE Trans. Cogn. Commun. Netw. **3**(4), 668–683 (2017)
15. An, K., Lin, M., Ouyang, J., Zhu, W.-P.: Secure transmission in cognitive satellite terrestrial networks. IEEE J. Sel. Areas Commun. **34**(11), 3025–3037 (2016)
16. Li, X., et al.: A unified framework for HS-UAV NOMA networks: performance analysis and location optimization. IEEE Access **8**, 13329–13340 (2020)
17. Zhang, X., et al.: Outage performance of NOMA-based cognitive hybrid satellite-terrestrial overlay networks by amplify-and-forward protocols. IEEE Access **7**, 85372–85381 (2019)
18. Xie, S., Zhang, B., Guo, D., Zhao, B.: Performance analysis and power allocation for NOMA-based hybrid satellite-terrestrial relay networks with imperfect channel state information. IEEE Access **7**, 136279–136289 (2019)

19. Zhu, Q., Wang, Y., Jiang, K., Chen, X., Zhong, W., Ahmed, N.: 3D non-stationary geometry-based multi-input multi-output channel model for UAV-ground communication systems. IET Microwaves Antennas Propag. **13**(8), 1104–1112 (2019)
20. Jiang, K., Chen, X., Zhu, Q., Chen, L., Xu, D., Chen, B.: A novel simulation model for nonstationary rice fading channels. Wirel. Commun. Mob. Comput. **2018**, 1–9 (2018)
21. Zhu, Q., et al.: A novel 3D non-stationary wireless MIMO channel simulator and hardware emulator. IEEE Trans. Commun. **66**(9), 3865–3878 (2018)
22. Zhu, Q., Liu, X., Yin, X., Chen, X., Xue, C.: A novel simulator of nonstationary random MIMO channels in Rayleigh fading scenarios. Int. J. Antennas Propag. **2016** 2016
23. Chen, X., Hu, X., Zhu, Q., Zhong, W., Chen, B.: Channel modeling and performance analysis for UAV relay systems. China Commun. **15**(12), 89–97 (2018)
24. Zhong, W., Xu, L., Zhu, Q., Chen, X., Zhou, J.: MmWave beamforming for UAV communications with unstable beam pointing. China Commun. **16**(1), 37–46 (2019)
25. Sharma, P.K., Deepthi, D., Kim, D.I.: Outage probability of 3-D mobile UAV relaying for hybrid satellite-terrestrial networks. IEEE Commun. Lett. **24**(2), 418–422 (2020)
26. Sharma, P.K., Kim, D.I.: Secure 3D mobile UAV relaying for hybrid satellite-terrestrial networks. IEEE Trans. Wirel. Commun. **19**(4), 2770–2784 (2020)
27. Qi, T., Feng, W., Wang, Y.: Outage performance of non-orthogonal multiple access based unmanned aerial vehicles satellite networks. China Commun. **15**(5), 1–8 (2018)
28. Loo, C.: A statistical model for a land mobile satellite link. IEEE Trans. Veh. Technol. **34**(3), 122–127 (1985)
29. Abdi, A., Lau, W.C., Alouini, M., Kaveh, M.: A new simple model for land mobile satellite channels: first- and second-order statistics. IEEE Trans. Wirel. Commun. **2**(3), 519–528 (2003)
30. Miridakis, N.I., Vergados, D.D., Michalas, A.: Dual-hop communication over a satellite relay and shadowed Rician channels. IEEE Trans. Veh. Technol. **64**(9), 4031–4040 (2015)
31. Upadhyay, P.K., Sharma, P.K.: Max-max user-relay selection scheme in multiuser and multirelay hybrid satellite-terrestrial relay systems. IEEE Commun. Lett. **20**(2), 268–271 (2016)
32. Gradshteyn, I.S., Ryzhik, I.M.: Table of Integrals, Series, and Products. Academic Press, Cambridge (2014)
33. Heath, R.W., Kountouris, M., Bai, T.: Modeling heterogeneous network interference using Poisson point processes. IEEE Trans. Signal Process. **61**(16), 4114–4126 (2013)